

Surface Enhanced Raman Scattering Investigation of the Halide Anion Effect on the Adsorption of 1,2,3-Triazole on Silver and Gold Colloidal Nanoparticles

Barbara Pergolese,^{*,†} Maurizio Muniz-Miranda,[‡] and Adriano Bigotto[†]

Department of Chemical Sciences, University of Trieste, Via L. Giorgieri 1, I-34127 Trieste, Italy, and
Department of Chemistry, University of Firenze, Via della Lastruccia 3, I-50019 Sesto Fiorentino, Italy

Received: January 10, 2005; In Final Form: March 22, 2005

The halide anion effect on the adsorption of 1,2,3-triazole on Ag and Au colloidal nanoparticles has been investigated by means of surface enhanced Raman scattering (SERS), UV–visible absorption spectroscopy, and scanning electron microscopy. To interpret the SERS spectra, the vibrational spectra of 1,2,3-triazole were assigned with the help of density functional theoretical (DFT) calculations of the two tautomers of 1,2,3-triazole, both free and bound to Ag and Au adatoms. Upon addition of halide anions, both tautomers interact with the Ag surface through one nitrogen atom. Analogous behavior is observed in the case of basified Au colloids, whereas at the usual pH of these hydrosols (~ 6) the adsorption of 1,2,3-triazole is the same of that observed in halide-free colloids.

Introduction

Since the very first SERS investigations in Ag hydrosols, a lot of interest arose about the influence of the addition of halide anions on SERS spectra. For most of the adsorbed molecules an increase of 2 or 3 orders of magnitude of the SERS signal is observed upon addition of the halide anions to silver colloids.^{1–4} It is necessary, however, that halide anions are specifically adsorbed on silver particles and this generally occurs for chloride, bromide, and iodide anions. Recently, this “activation” effect has been thoroughly investigated, because single-molecule SERS signals have been only detected in the case of activated silver colloids.^{5–10} Several explanations of the SERS activation due to the addition of halide anions were proposed,¹¹ essentially based on the formation of Ag^+ –halide–ligand surface complexes with a large charge transfer between adsorbate and metal or on the increase of the local electromagnetic field by aggregation of metal colloidal particles. Moreover, it is of note that both the adsorption mechanism and the surface coverage of an organic ligand¹² are strongly affected by the addition of halide anions. This could explain why the SERS spectra of some adsorbates are markedly enhanced by the addition of halide anions,^{1,11} whereas others are negatively affected by it.^{13–15}

The silver colloid activation is still a controversial point. Moreover, to the best of our knowledge, the effects produced by the addition of halide anions to gold colloids have never been studied before. Therefore, an investigation of the halide influence on the adsorption mechanism of a test compound, 1,2,3-triazole (hereafter TZ3), in Ag and Au hydrosols was considered of interest. This molecule has been chosen because we previously obtained and interpreted the SERS spectra of TZ3 in Ag and Au colloids without added halide anions.¹⁶

Because the coadsorption of halide anions affects both metal substrate and adsorbate,¹⁷ we have here investigated the

morphological changes of the metal substrates by scanning electron microscopy (SEM) and surface plasmon resonance (SPR) spectroscopy in the UV–visible region, whereas the modifications of the adsorbate have been evaluated on the basis of the SERS spectra. To give a firmer basis to the assignment of the SERS bands, a vibrational analysis of the IR and Raman spectra of TZ3 was performed, along with DFT calculations of the two tautomeric forms of TZ3, both free and bound to metal adatoms.

Experimental

TZ3 (97%) was obtained from Aldrich. Silver colloids were prepared following Creighton's procedure,¹⁸ by adding silver nitrate (Aldrich, purity 99.998%) to an aqueous solution of excess sodium borohydride (Aldrich, purity 99%) as reducing agent. The pH value of the silver colloidal dispersion was ~ 9 . Gold colloids were prepared according to the Turkevich's procedure,¹⁹ with excess sodium citrate (Aldrich, purity 99%). The pH value of the gold colloidal dispersion was ~ 6 . TZ3 was added to the metal colloidal suspensions to obtain 10^{-4} M concentrations. NaCl (Aldrich, purity 99.999%) or NaBr (Aldrich, purity 99.999%) was added in small amounts (10^{-3} M) to metal colloids, without modifying the sol stability.

The changes of the surface plasmon resonance bands of the silver and gold nanoparticles were monitored by UV–visible absorption spectra obtained with a UNICAM HeLios spectrophotometer and a Cary 5 spectrophotometer.

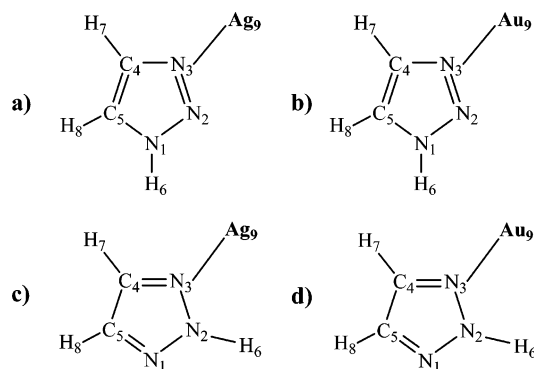
Microscopic measurements were performed by using a Quanta 200 ESEM (environmental scanning electron microscopy) instrument (FEY Company), operating in low-vacuum mode, and an electron beam emitted at 25 or 30 kV under 1 Torr (133 Pa) pressure. Solid-state backscatter detector (SSD-BSD) allowed collecting backscattered electrons emitted from the samples. These latter were constituted by drops of Ag colloids deposited as dry layers onto cover glasses.

SERS spectra in Ag colloids were recorded using the 514.5 nm line of a Coherent Argon ion laser or the 647.1 nm line of a Coherent Krypton laser, a Jobin-Yvon HG2S monochromator

* Corresponding author. E-mail: pergolese@dsch.univ.trieste.it. Telephone: +390405583950. Fax: +390405583903.

[†] University of Trieste.

[‡] University of Firenze.

CHART 1: Atomic Numbering of (A) 1H-TZ3/Ag, (B) 1H-TZ3/Au, (C) 2H-TZ3/Ag, and (D) 2H-TZ3/Au.

equipped with a cooled RCA-C31034A photomultiplier and a data acquisition facility. SERS spectra in Au colloids were obtained with a SPEX Ramalog instrument, controlled by an AT personal computer. Excitation was provided by the 647.1 nm line of a Spectra-Physics 165 Krypton ion laser. Total beam power was controlled at the sample using a power-meter model 362 (Scientech, Boulder, CO) giving $\sim 5\%$ accuracy in the 300–1000 nm spectral range.

The SERS enhancement factor depends on the concentration of the ligand really adsorbed on metal and on the shielding factor of the exciting and scattered radiations by colloidal metal particles.¹ By neglecting the possible changes of the adsorbate concentration by addition of halide anions, we performed a comparison between the SERS enhancements in the case of salt-free colloid and metal/halide colloid by estimating the intensity of the strongest SERS band with respect to the Raman intensity of the background. The changes of the shielding factor by addition of halide anions are expected to affect in the same way both the SERS signal of the ligand and Raman signal of the background.

Computational Details

Calculations of the two tautomers of 1,2,3-triazole (1H-TZ3 and 2H-TZ3, hereafter) and of their complexes with silver and gold adatoms were performed using the GAUSSIAN 98 package.²⁰ Optimized geometries were obtained at the density functional level of theory with the Becke's 1988 exchange functional in combination with the Perdew–Wang 91 gradient-corrected correlation functional. The calculations with this functional provided a satisfactory agreement between calculated and experimental wavenumbers without using scaling factors. The 6-31G** basis set was used for the calculations of both tautomers, whereas the LANL2DZ basis set for all the complexes. By allowing that all the parameters could relax, all the calculations converged to optimized geometries, which corresponded to true energy minima, as revealed by the lack of imaginary values in the wavenumber calculations. The atomic numbering of the models of surface complexes adopted in the calculations (hereafter 1H-TZ3/M, 2H-TZ3/M with M = Ag or Au) is shown in Chart 1. Harmonic vibrational wavenumbers were calculated at the same level of approximation using the parameters corresponding to the structure obtained from the optimization step. Force constants in internal coordinates, which were calculated according to the procedure described elsewhere,²¹ were used for a standard zero-order GF-matrix treatment from which vibrational wavenumbers and potential energy distributions (PEDs) were obtained. The Raman and IR wavenumbers of TZ3 are listed in Table 1, whereas in Table 2 the

TABLE 1: Experimental Wavenumbers of Liquid 1,2,3-Triazole

infrared	intensity	Raman	intensity
1527	m/s	1526	w
1444	m	1444	m
1420	m	1419	w/m
1384	w	1382	w
1342	vw	1333	vvw
—	—	1279	vw
1242	sh	1242	m/s
1224	s	1223	s
1175	w	1179	vs
		1148	s
~ 1130	sh	~ 1130	sh
1116	m		
1094	vs	1096	w
1072	vs	1073	w/m
972	m		
956	s	954	m
895	vw, br		
838	w		
790	vs	~ 800	vvw
702	w	706	vw
668	vvw	665	vw
636	vw	640	w

assignment of the vibrational bands to the calculated wavenumbers of 1H-TZ3 and 2H-TZ3 is reported, in comparison with the scaled MP2 values obtained by Törnkvist and co-workers.²² The calculated results of the models of surface complexes are reported in Tables 3 and 4, along with the SERS data.

Results and Discussion

UV–Visible Absorption Spectroscopy. As shown in Figure 1, the TZ3/Ag colloid exhibits a SPR band at 390 nm, ascribed to nonaggregated metal particles with spheroidal shape and 15 nm average diameter,²³ along with another broad band at about 570 nm, related to larger particles due to nanoparticle aggregation upon adsorption of TZ3. The addition of NaCl to the colloidal suspension promotes a further aggregation of the Ag nanoparticles, giving rise to a shoulder at about 430 nm, whereas the band at 570 nm becomes larger and shifts to greater wavelengths with a maximum centered at about 720 nm. A similar aggregation process can be proposed for the TZ3/Au colloids by the comparison of the visible absorption spectra before and after addition of NaCl (Figure 2). The SPR band at 520 nm is related to spheroidal gold nanoparticles, whereas that at 640 nm is related to aggregated metal particles with adsorbed TZ3. By addition of NaCl, this latter band becomes stronger and shifts to 715 nm, whereas the intensity of that at 520 nm decreases. These spectral evidences account for the increase of the percentage of the aggregated metal particles and of their average diameter in both silver and gold colloids.

Electron Microscopy. To obtain a direct evaluation of the particle aggregation process, microscopic measurements were performed with an ESEM (environmental scanning electron microscopy) instrument, by depositing and drying on glass some drops of the system constituted by the Ag colloid and TZ3, with or without chloride anions. As shown in Figure 3, the dark spots correspond to silver particles or aggregates. In the case of Ag colloids without Cl^- (upper image), spheroidal particles with diameters in the 100–400 nm range are observed. For Ag colloids with Cl^- (lower image), much larger Ag aggregates can be observed. Hence, these images show the increased aggregation of the Ag nanoparticles induced by the adsorption of chloride anions. Unfortunately, no microscopic measurement

TABLE 2: Experimental and Calculated Wavenumbers for 1H- and 2H-1,2,3-Triazole

1H-TZ3			2H-TZ3		
$\tilde{\nu}_{\text{obs}}^a$	$\tilde{\nu}_{\text{calc}}^b$ MP2/6-31G*	$\tilde{\nu}_{\text{calc}}^c$ BPW91/6-31G**	$\tilde{\nu}_{\text{obs}}^a$	$\tilde{\nu}_{\text{calc}}^b$ MP2/6-31G*	$\tilde{\nu}_{\text{calc}}^c$ BPW91/6-31G**
1527	1500 (A')	1501 (A')	1527	1482 (B ₂)	1497 (B ₂)
1444 ^d	1468 (A')	1427 (A')	1420	1443 (A ₁)	1417 (A ₁)
1342	1360 (A')	1340 (A')	1382 ^d	1403 (B ₂)	1369 (B ₂)
1242	1228 (A')	1240 (A')	1279 ^d	1277 (B ₂)	1258 (A ₁)
1179 ^d	1184 (A')	1157 (A')	1223 ^d	1258 (A ₁)	1229 (B ₂)
1094	1126 (A')	1099 (A')	1148 ^d	1152 (A ₁)	1149 (A ₁)
1072	1071 (A')	1077 (A')	1116	1116 (B ₂)	1103 (B ₂)
972	1041 (A')	995 (A')	1072	1094 (A ₁)	1071 (A ₁)
956	944 (A')	935 (A')	972	950 (A ₁)	952 (A ₁)
895	919 (A')	917 (A')	956	930 (B ₂)	932 (B ₂)
838	804 (A'')	821 (A'')	790	806 (B ₁)	812 (B ₁)
702	704 (A'')	707 (A'')	702	709 (B ₁)	705 (B ₁)
640 ^d	638 (A'')	641 (A'')	665 ^d	647 (A ₂)	660 (A ₂)

^a IR spectra. ^b Reference 33. ^c This work. ^d Raman spectra.

TABLE 3: SERS Data, Calculated Wavenumbers and Assignments for 1H-TZ3/Ag and 2H-TZ3/Ag

$\tilde{\nu}_{\text{obs}}^a$	$\tilde{\nu}_{\text{calc}}$ 1H-TZ3/Ag	PED ^b	$\tilde{\nu}_{\text{calc}}$ 2H-TZ3/Ag	PED ^b
1505	1497	36r _{4,5} , 17α _{6,1,5} , 14α _{6,1,2} , 8α _{8,5,1} , 7α _{7,4,3}		
1449			1463	15r _{4,3} , 9r _{1,5} , 25α _{6,2,3} , 24α _{6,2,1} , 7α _{7,4,5} , 5α _{7,4,3}
1416	1398	30r _{1,5} , 12r _{4,5} , 18α _{6,1,2} , 11α _{8,5,4} , 9α _{6,1,5} , 9α _{8,5,1}	1399	40r _{4,5} , 14α _{7,4,3} , 14α _{8,5,1} , 7α _{8,5,4} , 7α _{7,4,5}
1350	1348	16r _{4,3} , 5r _{4,5} , 19α _{7,4,3} , 18α _{7,4,5} , 12α _{6,1,2} , 10α _{6,1,5} , 7α _{8,5,4}	1341	11r _{5,1} , 10r _{4,3} , 20α _{6,2,1} , 20α _{6,2,3} , 11α _{8,5,4} , 7α _{7,4,5} , 6α _{8,5,1}
1270			1221	28r _{1,2} , 18r _{5,1} , 6r _{2,3} , 15α _{8,5,1} , 13α _{7,4,3} , 7α _{8,5,4} , 7α _{7,4,5}
1235			1214	49r _{4,3} , 27r _{5,1} , 6α _{1,2,3}
	1193	36r _{2,3} , 22r _{4,3} , 11r _{1,2} , 7α _{8,5,1} , 6α _{7,4,3}		
1168	1162	35r _{1,5} , 33r _{4,3} , 5r _{4,5} , 5α _{6,1,5} , 5α _{6,1,2} , 5α _{1,2,3}		
	1121	24r _{4,5} , 8r _{1,2} , 6r _{2,3} , 5r _{5,1} , 17α _{8,5,1} , 16α _{8,5,4} , 10α _{7,4,3} , 8α _{7,4,5}	1122	37r _{1,2} , 21r _{2,3} , 9r _{5,1} , 6r _{4,5} , 7α _{1,2,3} , 6α _{7,4,3}
1099			1092	34r _{4,5} , 17α _{8,5,4} , 17α _{8,5,1} , 8α _{7,4,5} , 7α _{7,4,3}
	1060	35r _{2,3} , 9r _{5,1} , 15α _{7,4,5} , 12α _{7,4,3} , 6α _{4,3,2}		
	1024	62r _{1,2} , 14α _{1,2,3} , 5α _{8,5,4}	1031	53r _{2,3} , 13r _{1,2} , 8α _{7,4,3} , 7α _{7,4,5}
988	958	15α _{1,2,3} , 12α _{8,5,1} , 10α _{4,3,2} , 10α _{8,5,4} , 8α _{6,1,5} , 8α _{5,1,2} , 8α _{7,4,5} , 8α _{5,4,3}	968	10r _{3,9} , 20α _{4,3,2} , 19α _{5,4,3} , 13α _{7,4,5} , 7α _{8,5,1} , 7α _{1,2,3}
	938	5r _{2,3} , 30α _{4,5,1} , 18α _{5,1,2} , 16α _{5,4,3} , 9α _{8,5,4} , 7α _{7,4,3} , 6α _{6,1,2}		
	878	34γ _{8,5} , 31γ _{7,4} , 24τ _{4,5} , 6τ _{5,1}	910	10r _{1,2} , 34α _{5,1,2} , 20α _{4,5,1} , 11α _{8,5,4} , 5α _{1,2,3}
			888	39γ _{8,5} , 30γ _{7,4} , 24τ _{4,5}
			823	47γ _{7,4} , 34γ _{8,5} , 9τ _{4,3} , 9τ _{5,1}
802	795	34γ _{7,4} , 29γ _{8,5} , 11γ _{6,1} , 17τ _{5,1} , 7τ _{4,3}		
	757	61γ _{6,1} , 8γ _{8,5} , 18τ _{1,2} , 9τ _{5,1}		
700			672	50τ _{1,2} , 16τ _{2,3} , 15γ _{6,2} , 8γ _{9,3}
653	659	45γ _{9,3} , 14γ _{6,1} , 19τ _{1,2} , 16τ _{2,3}	642	20γ _{9,3} , 8γ _{8,5} , 5γ _{7,4} , 29τ _{4,5} , 27τ _{5,1} , 5τ _{4,3}
	623	27γ _{6,1} , 5γ _{8,5} , 5γ _{7,4} , 5γ _{9,3} , 26τ _{4,5} , 16τ _{5,1} , 10τ _{1,2}		
			578	74γ _{6,2} , 6γ _{9,3} , 9τ _{2,3} , 6τ _{1,2}
215	215	94r _{3,9}	208	93r _{3,9}
	134	51α _{2,3,9} , 48α _{4,3,9}	154	50α _{2,3,9} , 48α _{4,3,9}
	118	60γ _{9,3} , 23τ _{4,3} , 17τ _{2,3}	103	61γ _{9,3} , 20τ _{2,3} , 18τ _{4,3}

^a SERS spectrum of TZ3/Ag colloid with 10⁻³ M NaCl. ^b r = stretching, α = in-plane bending, γ = out-of-plane bending, τ = torsion; only contributions ≥ 5 are reported (the numbering of the atoms corresponds to that reported in Chart 1).

of gold colloids could be obtained; however, it is reasonable to suppose that, upon addition of chloride anions, similar metal aggregates are formed, as suggested by the similar behavior of the SPR bands with respect to that shown in the case of Ag particles.

SERS Spectra in Ag Colloids. The SERS spectra of TZ3 in Ag and Au colloids without halide ions were previously recorded and interpreted.¹⁶ In Figure 4 the SERS spectra of TZ3 adsorbed on Ag colloids are reported. Upon addition of NaCl or NaBr to the Ag hydrosol, new bands appear in the SERS spectra and differences of the relative intensity of some bands are observed. Because these changes become more evident upon increasing the halide content (Figure 4B-D), the adsorption of a different species with respect to that in halide-free colloid is suggested. The formation of large Ag aggregates (see Figure 3) should

provide a further increase of the SERS signal by electromagnetic activation of the silver colloidal surface.²⁴ However, in the present case, upon addition of halide ions, the SERS enhancement does not significantly change.

The SERS spectrum in halide-free colloid (Figure 4A) exhibits few bands in the 600–1600 cm⁻¹ spectral region, due to the adsorption of the triazolate anion as a bidentate ligand. The occurrence of two distinct bands at 205 and 239 cm⁻¹, attributed to Ag–N stretching modes, accounts for the interaction of triazolate with Ag colloidal surface through two nitrogen atoms.¹⁶ Upon addition of NaCl or NaBr, both chloride and bromide anions strongly adsorb on silver, changing the SERS spectrum profile of the ligand. By adding NaCl, the band observed at ~240 cm⁻¹, attributable to the Ag–Cl stretching mode, masks the Ag–N stretching vibrations occurring in the

TABLE 4: SERS Data, Calculated Wavenumbers and Assignments for 1H-TZ3/Au and 2H-TZ3/Au

$\tilde{\nu}_{\text{obs}}^a$	$\tilde{\nu}_{\text{calc}}$ 1H-TZ3/Au	PED ^b	$\tilde{\nu}_{\text{calc}}$ 2H-TZ3/Au	PED ^b
1434	1504	38r _{4,5} , 16α _{6,1,5} , 13α _{6,1,2} , 8α _{8,5,1} , 7α _{7,4,3}	1462	18r _{4,3} , 8r _{5,1} , 25α _{6,2,3} , 22α _{6,2,1} , 6α _{7,4,5} , 5α _{8,5,4} , 5α _{7,4,3}
1416	1403	27r _{5,1} , 12r _{4,5} , 23α _{6,1,2} , 12α _{6,1,5} , 9α _{8,5,4} , 7α _{8,5,1}	1410	41r _{4,5} , 14α _{7,4,3} , 14α _{8,5,1} , 7α _{8,5,4} , 6α _{7,4,5}
1354	1354	18r _{4,3} , 18α _{7,4,5} , 18α _{7,4,3} , 9α _{8,5,4} , 8α _{6,1,5} , 8α _{6,1,2} , 6α _{8,5,1}	1336	11r _{5,1} , 9r _{4,3} , 5r _{1,2} , 22α _{6,2,3} , 20α _{6,2,1} , 11α _{8,5,4} , 7α _{7,4,5} , 6α _{8,5,1}
1236			1227	26r _{1,2} , 10r _{4,3} , 6r _{2,3} , 6r _{5,1} , 16α _{8,5,1} , 14α _{7,4,3} , 8α _{8,5,4} , 8α _{7,4,5}
1171	1207	30r _{4,3} , 25r _{2,3} , 15r _{1,2} , 7α _{8,5,1} , 5α _{7,4,3}	1226	37r _{4,3} , 33r _{5,1} , 7r _{1,2} , 9α _{1,2,3}
	1178	31r _{5,1} , 17r _{4,3} , 12r _{2,3} , 8r _{3,9} , 6r _{4,5} , 6α _{6,1,2} , 5α _{6,1,5}		
	1128	23r _{4,5} , 9r _{1,2} , 7r _{4,3} , 7r _{2,3} , 13α _{8,5,4} , 13α _{8,5,1} , 11α _{7,4,3} , 8α _{7,4,5}	1132	28r _{1,2} , 25r _{2,3} , 11r _{5,1} , 10r _{4,5} , 7α _{7,4,3}
1100			1100	30r _{4,5} , 6r _{1,2} , 6r _{5,1} , 17α _{8,5,1} , 16α _{8,5,4} , 8α _{7,4,5} , 6α _{7,4,3}
	1070	17r _{1,2} , 17r _{2,3} , 15r _{5,1} , 5r _{3,9} , 13α _{7,4,5} , 10α _{7,4,3} , 8α _{4,3,2}	1025	49r _{2,3} , 11r _{1,2} , 5r _{5,1} , 10α _{7,4,5} , 8α _{7,4,3}
	1030	40r _{1,2} , 19r _{2,3} , 9α _{1,2,3} , 7α _{7,4,5} , 6α _{8,5,1} , 6α _{8,5,4}	979	13r _{3,9} , 6r _{1,2} , 18α _{5,4,3} , 16α _{4,3,2} , 11α _{7,4,5} , 8α _{8,5,1} , 8α _{1,2,3}
984	964	10r _{4,3} , 19α _{1,2,3} , 10α _{8,5,1} , 9α _{4,3,2} , 9α _{6,1,5} , 8α _{5,1,2} , 7α _{8,5,4} , 7α _{5,4,3}		
948	934	10r _{2,3} , 29α _{4,5,1} , 17α _{5,1,2} , 13α _{5,4,3} , 9α _{8,5,4} , 8α _{7,4,3} , 5α _{6,1,2}	899	9r _{1,2} , 33α _{5,1,2} , 20α _{4,5,1} , 11α _{8,5,4} , 5α _{1,2,3}
	886	33γ _{8,5} , 32γ _{7,4} , 23τ _{4,5} , 6τ _{5,1}	896	36γ _{8,5} , 33γ _{7,4} , 23τ _{4,5}
	801	31γ _{7,4} , 25γ _{8,5} , 16γ _{6,1} , 19τ _{5,1} , 7τ _{4,3}	828	43γ _{7,4} , 37γ _{8,5} , 10τ _{5,1} , 9τ _{4,3}
	764	59γ _{6,1} , 12γ _{8,5} , 16τ _{1,2} , 7τ _{5,1}		
692			665	17γ _{6,2} , 6γ _{9,3} , 48τ _{1,2} , 18τ _{2,3} , 5τ _{5,1}
659	650	53γ _{9,3} , 10γ _{6,1} , 19τ _{1,2} , 13τ _{2,3}	636	27γ _{9,3} , 7γ _{6,2} , 7γ _{8,5} , 25τ _{4,5} , 22τ _{5,1} , 5τ _{4,3}
	621	26γ _{6,1} , 6γ _{9,3} , 6γ _{8,5} , 24τ _{4,5} , 17τ _{5,1} , 11τ _{1,2}		
255 ^c	261	90r _{3,9}	578	73γ _{6,2} , 8γ _{9,3} , 9τ _{2,3} , 5τ _{1,2}
	196	51α _{2,3,9} , 47α _{4,3,9}	257	87r _{3,9}
	164	59γ _{9,3} , 21τ _{4,3} , 19τ _{2,3}	196	49α _{2,3,9} , 46α _{4,3,9}
			150	61γ _{9,3} , 20τ _{2,3} , 19τ _{4,3}

^a SERS spectrum of TZ3/Au colloid with 10⁻³ M NaCl at pH 9. ^b r = stretching, α = in-plane bending, γ = out-of-plane bending, τ = torsion; only contributions ≥ 5 are reported (the numbering of the atoms corresponds to that reported in Chart 1). ^c SERS spectrum of TZ3/Au colloid with 10⁻³ M NaCl at pH 6.

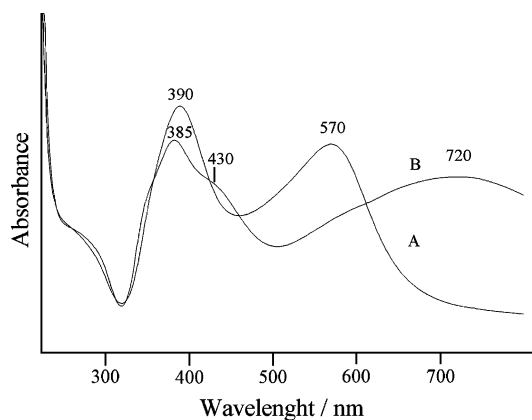


Figure 1. UV-visible absorption spectra of TZ3/Ag colloids without (A) and with (B) addition of 10⁻³ M NaCl.

same spectral region (spectra B and C). By addition of NaBr, instead, one Ag–N stretching band at ~215 cm⁻¹ (spectrum D) can be observed, not masked by the Ag–Br stretching mode occurring at about 160 cm⁻¹. This evidence suggests the presence of a single Ag–N bond but does not exclude the possibility of the overlapping of two bands or the presence of another Ag–N stretching band at lower wavenumbers, masked by the strong Ag–Br stretching mode. The other SERS bands closely correspond to those observed in Ag colloids with chloride anions (spectra B and C), where new bands at 988, 1270, 1350, 1416, and 1505 cm⁻¹ appear with respect to the spectrum A. Hence, upon addition of both chloride and bromide

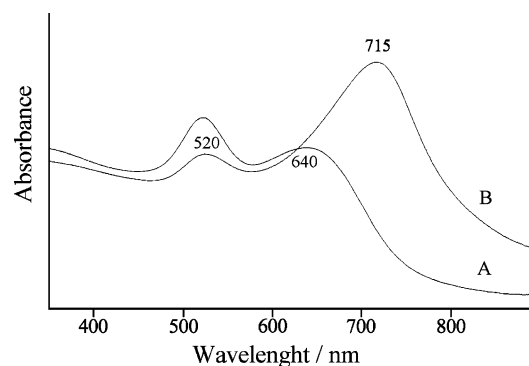


Figure 2. UV-visible absorption spectra of TZ3/Au colloids without (A) and with (B) addition of 10⁻³ M NaCl.

anions, the same adsorbate, different from that present in the case of halide-free Ag colloids, interacts with the metal surface.

The occurrence of new SERS bands of TZ3 is strictly dependent on the coadsorption of halide anions, because their intensities increase with the NaCl content (see spectra B and C). In particular, the band at 1505 cm⁻¹ can be confidently assigned to the N–H bending mode of TZ3. Thus, it can be deduced the halide addition induces the adsorption of TZ3 as neutral molecule, as found in the case of 2-amino-5-nitropyridine.²⁵ In fact, the pH of Ag colloids prepared with borohydride is alkaline (~9) and hydroxide anions adsorb on the silver surface. Because these anions promote the deprotonation of the organic ligand, TZ3 adsorbs in the anionic form. On the other hand, chloride or bromide anions are able to remove hydroxide

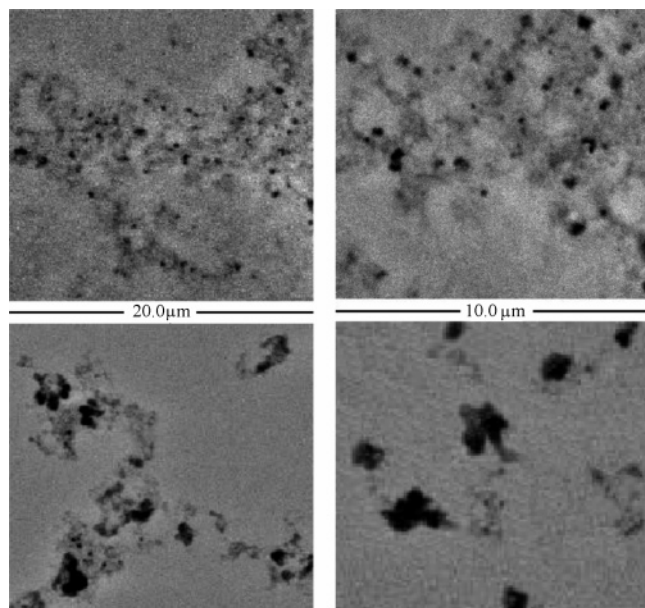


Figure 3. ESEM images of TZ3/Ag colloids: without halide ions (above); with 10^{-3} M NaCl (below).

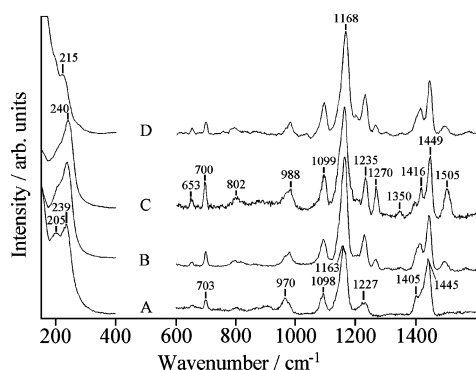


Figure 4. SERS spectra of TZ3/Ag colloids: (A) without halide ions; (B) with 10^{-3} M NaCl; (C) with 2×10^{-3} M NaCl; (D) with 10^{-3} M NaBr. Exciting line: 514.5 nm.

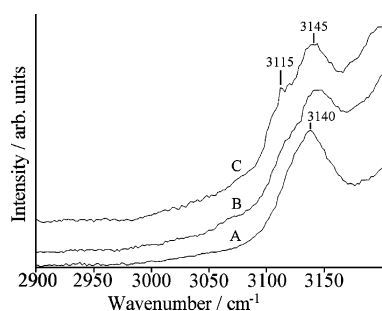


Figure 5. SERS spectra of TZ3/Ag colloids in the 2900–3200 cm^{-1} spectral region: (A) halide-free Ag colloid; (B) Ag colloid with 10^{-3} M NaCl; (C) Ag colloid with 10^{-3} M NaBr. Exciting line: 514.5 nm.

ions from the silver surface,^{25,26} favoring the adsorption of the ligand as neutral molecule.

The SERS spectra in the 2900–3200 cm^{-1} region (Figure 5) confirm that TZ3 adsorbs in the neutral form in Ag/halide colloids. In fact, in halide-free colloids only a strong band is observed around 3140 cm^{-1} (spectrum A), due to the C–H stretching mode. This band shifts to 3145 cm^{-1} by addition of halide anions (spectra B and C), along with the appearance of a shoulder at ~ 3115 cm^{-1} . This latter band does not likely correspond to the N–H stretching vibration of TZ3, because this mode is not usually observed in SERS spectra in colloids,

but to a different C–H stretching vibration. As previously ascertained,¹⁶ in halide-free Ag hydrosol the triazolate anion adsorbs as bidentate ligand, maintaining C_{2v} symmetry; hence, only one totally symmetric C–H stretching mode occurs in the SERS spectrum. If, upon addition of halide anions, the neutral TZ3 interacts with silver through only one nitrogen atom, the symmetry of the surface complex is lowered to C_s and two totally symmetric C–H stretching modes can be observed in the SERS spectrum.

To interpret the SERS spectra of TZ3, the IR and Raman bands of this compound should be correctly assigned. The vibrational analysis of this molecule is strongly complicated by the presence of two tautomers: 1H-1,2,3-triazole (1H-TZ3) with C_s symmetry and 2H-1,2,3-triazole (2H-TZ3) with C_{2v} symmetry. 1H-TZ3 was considered the dominant form in the gas phase from infrared²⁷ and microwave²⁸ spectroscopies, even if Begtrup et al.²⁹ showed that 2H-TZ3 was largely predominant by a combined study of microwave spectroscopy, gas-phase electron diffraction and ab initio calculations. The coexistence of the two tautomers is proposed in solution^{30–32} as well as in the liquid.³³ In the crystalline phase the contemporary presence of the two forms is also obtained by X-ray diffraction.³⁴ Until now, an exhaustive vibrational assignment of the infrared and Raman bands of the two tautomers has not been proposed, even if some experimental and theoretical studies were performed.^{33,35} The Raman bands in aqueous solution closely match those in the liquid, even if some differences occur in the relative intensities.

DFT calculations have been here carried out for both tautomeric forms of TZ3. The comparison between these results and the scaled MP2 wavenumbers obtained by Törnkvist et al.³⁰ has been also performed: our calculated wavenumbers provide a better agreement with the experimental data without using scaling factors. The assignment proposed by Keresztury and co-workers³³ has not taken into account, because they did not consider the intense Raman bands at 1179 and 1148 cm^{-1} . In the present assignment the vibrational bands observed at 1444, 1242, 1179, 1094, and 640 cm^{-1} are attributed to 1H-TZ3, whereas those at 1420, 1382, 1279, 1223, 1148, and 665 cm^{-1} to 2H-TZ3. The vibrational bands at 1527, 1072, 956, and 702 cm^{-1} are attributable to both tautomers. Hence, it can be deduced that both 1H- and 2H-TZ3 are present in the liquid, even if their percentages cannot be evaluated.

All the SERS bands of TZ3 in Ag colloids with halide anions can be attributed to fundamentals of the neutral molecule, adsorbed as 1H-TZ3 or 2H-TZ3. For example, the SERS band at 1505 cm^{-1} corresponds to the IR band at 1527 cm^{-1} , attributable to N–H bending mode, whereas those at 1416, 1350, and 1270 cm^{-1} can be related to the vibrational bands at 1420, 1342, and 1279 cm^{-1} assigned to ring stretching modes.

SERS Spectra in Au Colloids. The addition of chloride anions to TZ3/Au colloids does not cause a significant increase in the SERS enhancement, as in the case of the Ag hydrosols, in contrast with the aggregation of the gold particles observed in the visible absorption spectra (Figure 2). To obtain a satisfactory SERS effect from Au colloids, a red-shifted laser line (647.1 nm) has been employed, to match the surface plasmon resonance bands of the gold nanoparticles (Figure 2). In Figure 6 the SERS spectra of TZ3 in Au colloids are compared with those obtained in Ag hydrosol by excitation with 647.1 nm laser line.

The SERS spectra in Ag colloids with chloride anions, by excitation with the laser line at 647.1 nm (Figure 6A), does not show the occurrence of the bands at about 1270 and 1505 cm^{-1} ,

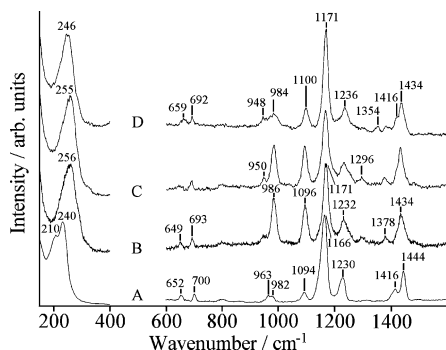


Figure 6. (A) SERS spectrum of TZ3/Ag colloid with 10^{-3} M NaCl; (B) SERS spectrum of TZ3/Au colloid without addition of halide ions (pH 6); (C) SERS spectrum of TZ3/Au colloid with 10^{-3} M NaCl (pH 6); (D) as (C), but at pH 9. Exciting line: 647.1 nm.

which, instead, are observed by excitation with 514.5 nm laser line (Figure 4). This could be explained by considering that these bands are assigned to Raman-active modes without an appreciable value of α_{zz} (where z is the axis normal to the metal surface), as expected on the basis of the electromagnetic enhancement effect by using red-shifted exciting lines.³⁵ The SERS spectra obtained in Au hydrosols without or with addition of chloride anions are very similar, but markedly different from the SERS spectrum in Ag hydrosol: the bands at 986 and 1096 cm^{-1} are stronger, whereas that at about 1416 cm^{-1} does not occur. It is of note that the pH of the gold colloids is ~ 6 . However, by basifying the Au aqueous dispersion to the pH value of the Ag colloids (~ 9), the SERS spectrum becomes comparable with that in Ag colloid, where the adsorption of the neutral molecule was above ascertained. However, the similarity between the SERS spectra of TZ3/Au colloids at pH ~ 6 , without and with chloride anions, suggests that in both samples triazolate adsorbs on gold as bidentate ligand.¹⁶ In these spectra a strong band occurs at about 255 cm^{-1} , attributable to the Au–N stretching vibration. At pH ~ 9 the Au–N stretching band is masked by the Au–Cl stretching band, which falls at about 240 cm^{-1} , as in the case of Ag colloids. These evidences suggest that chloride anions do not adsorb on gold colloidal nanoparticles at acidic pH values and, thus, they cannot affect the adsorption of TZ3, which interacts with the gold surface in the anionic form, as in chloride-free colloids. At alkaline pH, instead, TZ3 adsorbs as neutral molecule by effect of coadsorbed chloride anions and, thus, the SERS in Au hydrosols closely correspond to that in Ag hydrosols.

Calculations of TZ3/Metal Models. The calculations of surface complexes constituted by molecules bound to metal adatoms provide useful information about the interaction between adsorbate and metal substrate.^{16,21,36} The existence of two tautomers of TZ3 and the possibility of interaction with one or two surface metal sites with different electric charges make the SERS interpretation complicated. Hence, DFT calculations have been performed on models of 1H-TZ3 and 2H-TZ3 bound to one or two Ag^+ , because the surface Ag sites are to be considered positively charged by effect of coadsorbed halide anions.^{17,37} On the basis of these calculations the possibility of interaction with two silver sites is ruled out for both tautomers. In fact, no energy minimum was found for the model of 1H-TZ3 bound to two Ag^+ and the calculated wavenumbers for the complex of 2H-TZ3 coordinated to two Ag^+ do not agree with the experimental data.

Therefore, the complexes of the two tautomers with only one Ag^+ were considered reliable adsorption models of 1H-TZ3 and 2H-TZ3 on silver (see Chart 1). In the case of 1H-TZ3, the

interaction with the silver ion is only possible through the N_3 nitrogen atom. The wavenumbers of the SERS bands are satisfactorily reproduced by the calculated wavenumbers of the two tautomers, as shown in Table 3. The SERS bands at 1168 and 1505 cm^{-1} are attributed to 1H-TZ3. For this latter band the contribution of the N–H in-plane bending mode is sizable, as expected. On the contrary, the SERS bands at 1449 and 1099 cm^{-1} are attributed to 2H-TZ3. The Ag–N stretching band is well reproduced by the calculations for both tautomers bound to one silver ion. This observation is in agreement with the occurrence of a single SERS band at $\sim 215 \text{ cm}^{-1}$. As a conclusion, the several SERS bands observed in Ag/halide hydrosols are due to the adsorption of both tautomers of TZ3, as above suggested by experimental evidences, even if the presence of adsorbed triazolate, as minority species, cannot be completely excluded.

As shown in Figure 6, the SERS spectra of TZ3 adsorbed on Au/halide colloids at alkaline pH are quite similar to the corresponding spectra in silver hydrosols. Hence, it is reasonable to suppose that TZ3 interacts with the gold substrate in a similar way. The calculations, performed on TZ3/Au complexes, confirm this hypothesis: the adsorption of TZ3 on gold is satisfactorily mimicked by the model constituted by 1H- or 2H-TZ3 bound to one positively charged gold adatom.

Conclusions

The halide anion effect on the adsorption of TZ3 onto silver and gold colloidal nanoparticles has been investigated by means of surface plasmon resonance spectroscopy, scanning electron microscopy and surface-enhanced Raman scattering. DFT calculations of the free molecule and of surface complex models of TZ3 bound to silver or gold adatoms help the assignments of the vibrational and SERS spectra.

Aggregation of the silver and gold nanoparticles upon addition of halide anions has been observed by microscopic and UV–visible absorption measurements. However, no significant increase in the SERS enhancement of TZ3 has been detected in both silver and gold hydrosols by addition of chloride or bromide anions, as, instead, expected on the basis of the electromagnetic mechanism after colloidal aggregation. In the case of Au hydrosols at their usual pH (~ 6), no difference is observed between the SERS spectra with or without halide addition. In the case of silver and basified gold colloids, instead, the presence of coadsorbed halide anions induces the adsorption of TZ3 as neutral molecule through one nitrogen atom. The occurrence of several bands in the SERS spectra of TZ3 adsorbed on Ag/halide or Au/halide colloids is due to the adsorption of both tautomers of TZ3, as deduced by the spectral and computational results.

Acknowledgment. We gratefully thank the Italian Ministero dell'Istruzione, Università e Ricerca (MIUR) for the financial support and Prof. Elena Bonzi (CEME, CNR) for her help in the microscope measurements.

References and Notes

- (1) Hildebrandt, P.; Stockburger, M. *J. Phys. Chem.* **1984**, *88*, 5935.
- (2) Hildebrandt, P.; Keller, S.; Hoffmann, A.; Vanhecke, F.; Schrader, B. *J. Raman Spectrosc.* **1993**, *24*, 791.
- (3) Wehling, B.; Hill, W.; Klockow, D. *J. Mol. Struct.* **1995**, *349*, 117.
- (4) Schneider, S.; Grau, H.; Halbig, P.; Freunscht, P.; Nickel, U. *J. Raman Spectrosc.* **1996**, *27*, 57.
- (5) Kneipp, K.; Wang, Y.; Kneipp, H.; Perelman, L. T.; Itzkan, I.; Dasari, R.; Feld, M. S. *Phys. Rev. Lett.* **1997**, *78*, 1667.
- (6) Nie, S.; Emory, S. R. *Science* **1997**, *275*, 1102.

- (7) Bosnick, K. A.; Jiang, J.; Brus, L. E. *J. Phys. Chem. B* **2002**, *106*, 8096.
- (8) Futamata, M.; Maruyama, Y.; Ishikawa, M. *Vibr. Spectrosc.* **2002**, *30*, 17.
- (9) Doering, W. E.; Nie, S. *J. Phys. Chem. B* **2002**, *106*, 311.
- (10) Otto, A.; Bruckbauer, A.; Chen, Y. X. *J. Mol. Struct.* **2003**, *661*–662, 501.
- (11) Grochala, W.; Kudelski, A.; Bukowska, J. *J. Raman Spectrosc.* **1998**, *29*, 681.
- (12) Sánchez-Cortés, S.; García-Ramos, J. V. *Surf. Sci.* **2001**, *473*, 133.
- (13) Campbell, M.; Lecompte, S.; Smith, W. E. *J. Raman Spectrosc.* **1999**, *30*, 37.
- (14) Fu, S.; Zhang, P. *J. Raman Spectrosc.* **1992**, *23*, 93.
- (15) Fang, Y. *J. Raman Spectrosc.* **1999**, *30*, 85.
- (16) Pergolese, B.; Muniz-Miranda, M.; Bigotto, A. *J. Phys. Chem. B* **2004**, *108*, 5698.
- (17) Muniz-Miranda, M.; Sbrana, G. *J. Raman Spectrosc.* **1996**, *27*, 105.
- (18) Creighton, J. A.; Blatchford, C. G.; Albrecht, M. G. *J. Chem. Soc., Faraday Trans. 2* **1979**, *75*, 790.
- (19) Turkevich, J.; Stevenson, P. C.; Hillier, J. *J. Discuss. Faraday Soc.* **1951**, *11*, 55.
- (20) Frisch, M. J.; Trucks, G. W.; Schlegel, H. B.; Scuseria, G. E.; Robb, M. A.; Cheeseman, J. R.; Zakrzewski, V. G.; Montgomery, J. A., Jr.; Stratmann, R. E.; Burant, J. C.; Dapprich, S.; Millam, J. M.; Daniels, A. D.; Kudin, K. N.; Strain, M. C.; Farkas, O.; Tomasi, J.; Barone, V.; Cossi, M.; Cammi, R.; Mennucci, B.; Pomelli, C.; Adamo, C.; Clifford, S.; Ochterski, J.; Petersson, G. A.; Ayala, P. Y.; Cui, Q.; Morokuma, K.; Malick, D. K.; Rabuck, A. D.; Raghavachari, K.; Foresman, J. B.; Cioslowski, J.; Ortiz, J. V.; Stefanov, B. B.; Liu, G.; Liashenko, A.; Piskorz, P.; Komaromi, I.; Gomperts, R.; Martin, R. L.; Fox, D. J.; Keith, T.; Al-Laham, M. A.; Peng, C. Y.; Nanayakkara, A.; Gonzalez, C.; Challacombe, M.; Gill, P. M. W.; Johnson, B.; Chen, W.; Wong, M. W.; Andres, J. L.; Gonzalez, C.; Head-Gordon, M.; Replogle, E. S.; Pople, J. A. *GAUSSIAN 98*, revision A.6.; Gaussian Inc.: Pittsburgh, PA, 1998.
- (21) Pergolese, B.; Bigotto, A. *Spectrochim. Acta A* **2001**, *57*, 1191.
- (22) Törnkvist, C.; Bergman, J.; Liedberg, B. *Phys. Chem.* **1991**, *95*, 3123.
- (23) Nabiev, I. R.; Savchenko, V. A.; Efremov, E. S. *J. Raman Spectrosc.* **1983**, *14*, 375.
- (24) Grochala, W.; Kudelski, A.; Bukowska, J. *J. Raman Spectrosc.* **1998**, *29*, 681.
- (25) Muniz-Miranda, M.; Neto, N.; Sbrana, G. *J. Mol. Struct.* **1995**, *348*, 261.
- (26) Park, H.; Lee, S. B.; Kim, M. S.; Kim, K. *Chem. Phys.* **1992**, *161*, 265.
- (27) Borello, E.; Zecchina, A.; Guglielminotti, E. *J. Chem. Soc. B* **1969**, 307.
- (28) Stiefvater, O. L.; Jones, H.; Sheridan, J. *Spectrochim. Acta A* **1970**, *26*, 825.
- (29) Begtrup, M.; Nielsen, C. J.; Nygaard, L.; Samdal, S.; Sjøgren, C. E.; Sørensen, G. O. *Acta Chem. Scand. A* **1988**, *42*, 500.
- (30) Albert, A.; Taylor, P. J. *J. Chem. Soc., Perkin Trans. 2* **1989**, 1903.
- (31) Catalán, J.; Sánchez-Cabezudo, M.; de Paz, J. L. G.; Elguero, J.; Taft, R. W.; Anvia, F. *J. Comput. Chem.* **1989**, *10*, 426.
- (32) Cox, J. R.; Woodcock, S.; Hillier, I. H.; Vincent, M. A. *J. Phys. Chem.* **1990**, *94*, 5499.
- (33) Billes, F.; Endrédi, H.; Keresztury, G. *J. Mol. Struct. (THEOCHEM)* **2000**, *530*, 183.
- (34) Godard, R.; Heinemann, O.; Krüger, C. *Acta Crystallogr. C* **1997**, *53*, 1846.
- (35) Moskovits, M.; Suh, J. S. *J. Phys. Chem.* **1984**, *88*, 5526.
- (36) Cardini, G.; Muniz-Miranda, M. *J. Phys. Chem. B* **2002**, *106*, 6875.
- (37) Wetzell, H.; Gerischer, H. *Chem. Phys. Lett.* **1980**, *76*, 460.